CANCOM2024 – CANADIAN INTERNATIONAL CONFERENCE ON COMPOSITE MATERIALS

ANALYSIS OF THE INTERFACE PROPERTIES OF MULTI-MATERIAL FUSED FILAMENT FABRICATED (FFF) PRINTED STRUCTURES

Pahari, Shauvik[1] and Melenka, Garrett W.[1]*
[1] Mechanical Engineering, York University, Toronto, Canada
* Corresponding author (gmelenka@yorku.ca)

Keywords: *Multi-material 3D printing, Fused Filament Fabrication, Digital Image Correlation, Lap-shear*

ABSTRACT

Advancements in 3D printing technology and a wider range of available materials have led to increased research on multi-material 3D printing. There has been limited exploration within Fused Filament Fabrication (FFF), a method widely adopted in 3D printing. The ability of multi-material 3D printing to enable the fabrication of objects with enhanced functionality and to allow tailoring of the mechanical properties according to specific applications has prompted significant interest. This paper addresses the mechanical performance of multi-material 3D printed structures, primarily focusing on the interface between two polymers at their geometrical boundaries. Two filaments were used for this study: i) Polyethylene terephthalate glycol (PETG) and ii) Polyethylene terephthalate glycol mixed with 20% short carbon fibers (PETC). A PETG-PETG lap joint, PETC-PETC lap joint, and PETG-PETC lap joint were fabricated using the Prusa MK3S with multi-material unit (MMU2) attachment. A universal testing machine conducted the lap shear test on the three structures. The boundary region of the lap joint between the two polymers has been analyzed using a 2D Digital Image Correlation (DIC). This DIC analysis helped in an in-depth understanding of the interface between the different materials at their geometrical boundaries, which is deemed crucial for assessing the feasibility of multi-material 3D printing. The findings show that the heterogenous PETG-PETC exhibits higher strength compared to the homogenous samples.

1 INTRODUCTION

One of the key topics of the 21st century in our society is sustainability. Industrial activity accounts for 22% of total final energy consumption and for about 20% of global CO2 emissions [1]. According to the model calculations shown by Gebler et al., 3D Printing has the potential to reduce costs by 170-593 billion US $, the total primary energy supply by 2.54-9.30 EJ, and CO2 emissions by 130.5-525.5 Mt by 2025 [2]. Until recently, studies have focused on single-material solutions, even after the advent of multi-material 3D printing technologies. One of the main reasons for limited exploration of multi-material 3D printing is the high price of the multi-material printers [3].

3D printing of multi-material components has enabled manufacturing of 3D printed parts with enhanced functionality [4,5], reduced part components, and streamlined assembly. This technology enables to selectively design samples with multiple materials with varying mechanical properties, offering design freedom to manufacture parts with enhanced mechanical properties [6,7] and fracture resistance [8]. The challenge with 3D printing processes is the porosity and anisotropy associated with layer-by-layer printing process. This can lead to weak layer adhesion, which results in reduced strength [9].

Some studies [10,11] have been conducted to investigate the boundary interface of multi-material Fused Filament Fabrication (FFF) printed structures, where the most used filaments like PLA and TPU were used with more

focus on different interlocking mechanisms. But the strength of the multi-materials was significantly less compared to the homogenous samples.

This study aims to analyze the interface between the multi-material structures in the form of lap joints and explore more unconventional materials. Test specimens were manufactured by FFF and tested in a universal testing machine. 2D Digital Image Correlation (DIC) was conducted to evaluate the mechanical properties of the manufactured specimens, which allowed for the visualization of strain localization on the samples and aided in predicting points of failure. The results demonstrate the feasibility of FFF multi-material printing, highlighting the capability of desktop FFF printers to manufacture composites with enhanced mechanical properties and the added benefit of the versatility offered by 3D printing.

2 EXPERIMENTAL METHODS

2.1 Sample manufacturing:

The single lap joints as shown in Figure 1 were designed using SolidWorks (Dassault Systèmes SolidWorks Corporation, Massachusetts, USA) for a standard test method for lap shear adhesion for fiber-reinforced plastic (FRP) bonding [12]. The lap shear overlap area is 6.45 cm^2 (1 $inch^2$), but the samples' thickness had to be reduced to 2.35 mm from 2.5 mm so that the samples could fit into the clamps of the universal testing machine. All the samples were fabricated using the open-source FFF 3D printer (Prusa mk3S, Prusa Research, Prague, Czech Republic). Multi Material Upgrade 2.0 (MMU2) (Prusa Research, Prague, Czech Republic) was also attached to the printer to allow the printer to print with multiple filaments at the same time. The design of the MMU2 had a limitation where it did not support printing different materials if the materials have a different printing temperature. So, custom G-codes were added in the slicer software (Prusa Slicer, Prusa Research, Prague, Czech Republic) to change the extruder temperature before the second filament is introduced in the extruder.

Table 1. 3D printing parameter for the lap joints

Parameters	Value	Units
Nozzle diameter	0.4	mm
Extruder temperature (PETG)	230	°C
Extruder temperature (PETC)	230	°C
Printer bed temperature (PETG & PETC)	85	°C
Printing speed	45	mm/s
Infill densities	100	%
Layer height	0.2	mm

2.2 Materials:

PETG is one of the most commonly used thermoplastic filaments which is used in clothing and food packaging applications. PETC has been used to investigate the effect of fibers on the adhesion of the multi-material specimen at the interface. Two different filaments of diameter 1.75 mm – a) PETG (Eryone, Guandong, China) and b) PETC (iSANGHU, Guandong, China) were used as polymer feedstock to print the different sample combinations. These two filaments were used to print three different specimen combinations: i) PETG-PETG, ii) PETC-PETC, and iii) PETG-PETC (Figure 1).

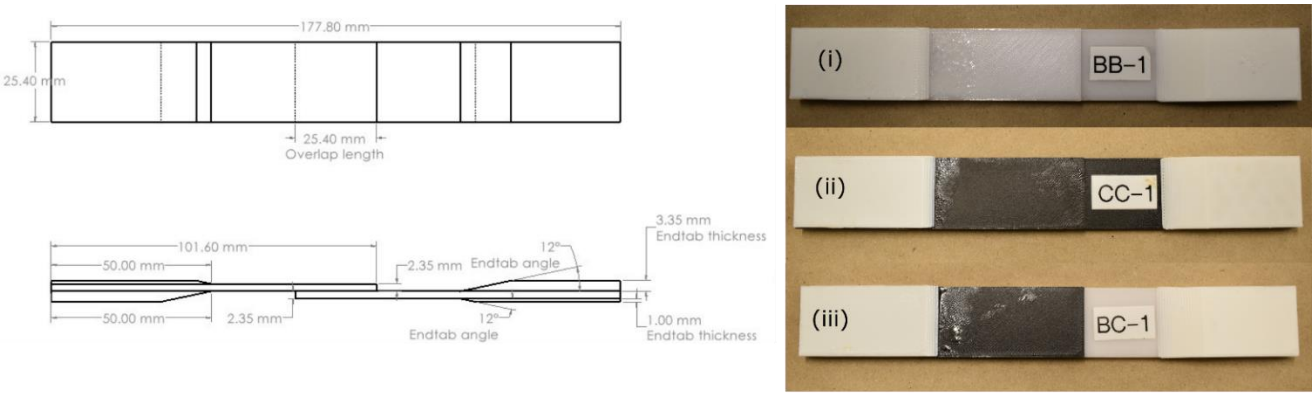

Figure 1: (a) Schematic of specimen geometry. (b) Specimens with endtabs: i) PETG-PETG, ii) PETC-PETC, and iii) PETG-PETC

2.3 Sample preparation for DIC:

End tabs were attached to the specimens to allow for the shear load to be applied to the specimens. The end tabs were bonded using a high strength two-part epoxy (Gorilla Epoxy, Gorilla Glue Company, Cincinnati, OH). All the samples were painted with matte black spray paint (Painter's Touch Flat Black, Rust-Oleum Corp., Concord, ON) to improve the contrast for 2D DIC measurement. Next, a mixture of white paint (5212 Opaque White, Createx Airbrush Colors, Createx Colors, East Granby CT) and reducer (4012 High Performance Reducer, Createx) is applied to the sample with an airbrush (Paasche Airbrush H-3MH set, Paasche Airbrush Co, Chicago, IL) for a white speckle pattern.

2.4 Shear test:

Tensile loads were applied to the braid samples using a universal testing machine (ElectroPuls® E3000, Instron, Norwood, USA) equipped with a 3 kN load cell. The specimens were loaded at a constant rate of 1mm/min. The load rate was chosen to get optimum images for accurate DIC processing. The output channel (load channel) from the analog I/O port of the rear panel of the Instron controller was connected to the analog-to-digital converter (ADC) in the LaVision system for synchronization.

2.5 2D DIC imaging setup:

Two high-resolution cameras (Imager M-lite 5M, LaVision GmbH, Göttingen, Germany) were placed at 90° to each other to image both the front and side views of the sample. Images were acquired at a rate of 20 frames per second. The camera and image properties have been listed in Table 3. The camera for imaging the wider front view was equipped with a fixed focal length lens (MVL50M23 50 mm, Navitar, Rochester, USA), and the camera for imaging the narrower side view was equipped with a macro lens (3.3X macro zoom, Edmund Optics, Barrington, USA).

Table 2: Camera and image properties for DIC imaging

Property	Unit	Value
Camera resolution	px x px	2464 x 2056
Pixel size	µm	3.45
Frame rate	Hz	20
Image Scaling Factor (50 mm lens)	px/mm	27
Image Scaling Factor (macro lens)	px/mm	1611
Image field of view (50 mm lens)	mm x mm	90 x 60
Image field of view (macro lens)	mm x mm	15 x 5

2.6 2D DIC processing:

All the acquired images were processed using a commercial image processing software (Davis version 10.2 Strainmaster, LaVision GmbH, Göttingen, Germany) to measure the displacement and strain of the lap joint specimens. The images collected with the 50 mm lens were calibrated using a two-level 3D calibration plate (Type 058-5-SSDP, LaVision GmbH, Göttingen, Germany) while the images with the macro lens were scaled using a steel ruler (182-105, Mitutoyo Canada Inc., Mississauga, ON). The specimen images with the 50 mm lens were processed with a subset size of 15 pixels and a step size of 7 pixels. On the contrary, the specimen images with the macro lens were processed with a subset size of 25 pixels and a step size of 12 pixels.

3 RESULTS AND DISCUSSIONS:

3.1 DIC strain maps of the different samples

The axial strain maps on the front side for all the different specimens are shown in Figure 2. The multi-material PETG-PETC specimen fails at a higher load than the homogenous specimens. The strain map shows the strain localization at the top and bottom of the overlap region, after which it fails at the top or bottom of the overlap region. Notably, the multi-material specimen does not delaminate at the interface or undergo cohesive failure. The PETC-PETC also has higher strength than the PETG-PETG specimen due to the presence of short carbon fibers, which helps with better adhesion.

The shear strain maps on the side view for all the specimens in Figure 3 It also shows that the shear strain is localized more at the bottom of the overlap region. The multi-material specimen also shows similar strain propagation to the homogenous specimens. It does not propagate along the joint's interface, hence showing reduced chances of delamination at the interface. All these results show that the heterogenous PETG-PETC specimens have the highest strength.

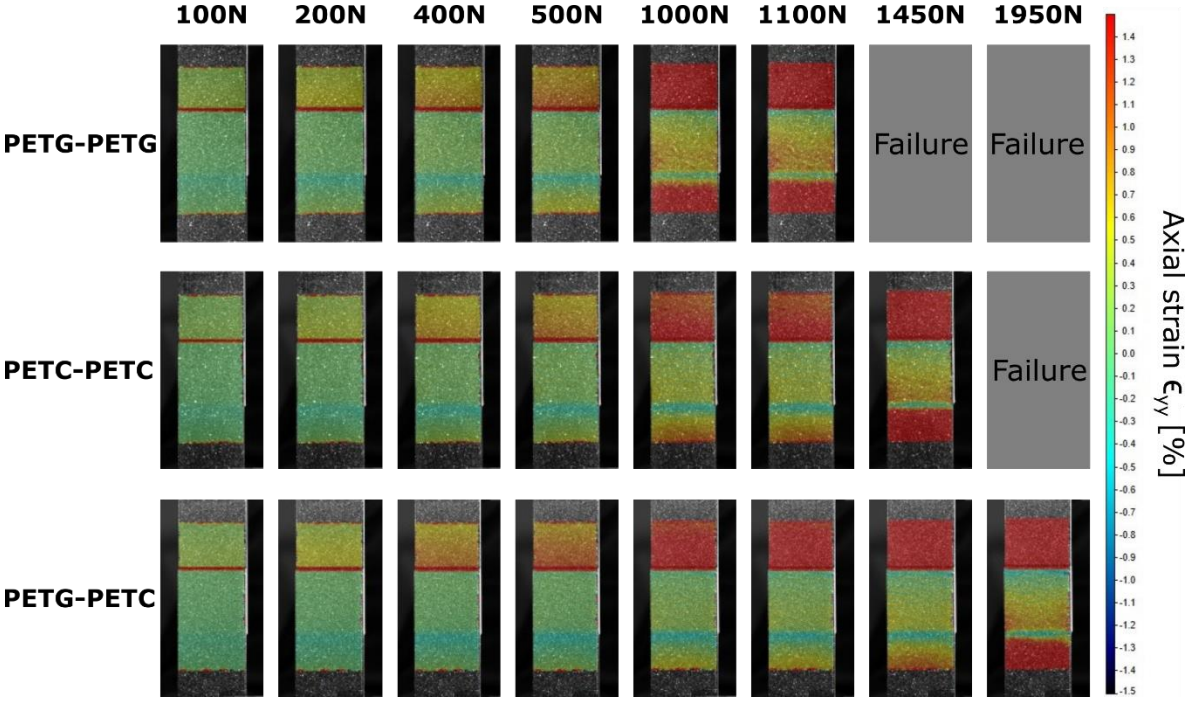

Figure 2: Comparison of axial strain for all the different samples (front view) under different loads

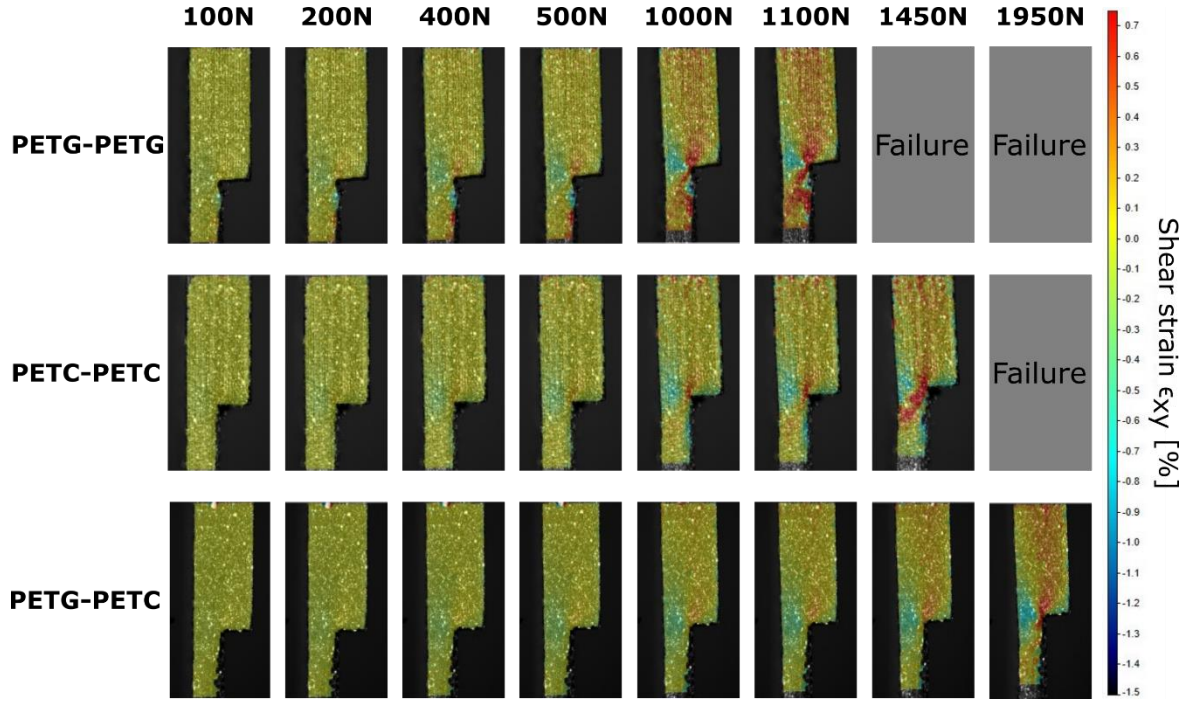

Figure 3: Comparison of shear strain for all different samples (side view) under different loads

3.2 Load-displacement curve

The resulting load-displacement curves can be seen in Figure 4. The short carbon fibers in homogenous PETC improve the strength of the specimens compared to homogenous PETG samples and fail at a higher load around 1500N. Surprisingly, the heterogenous PETG-PETC samples have higher shear strength than the homogenous samples. This can be attributed to the presence of the short carbon fibers on one side of the interface in the overlap region, which has a Velcro-like effect.

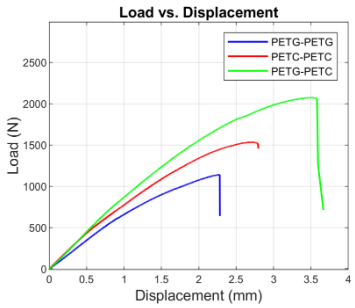

Figure 4: Load versus displacement curves for different specimens.

4 CONCLUSION

The homogenous and the multi-material lap joints were manufactured with FFF printing process. All the specimens were evaluated using shear test and 2D DIC technique was used for detailed analysis of the mechanical behavior of the specimens. The results demonstrate the effect of boundary interface in the lap joints for better adhesion. The result shows that the multi-material PETG-PETC lap joint has higher shear strength than the homogenous specimens. Thus, introducing fibers in the filaments can improve the adhesion of the multi-materials at the boundary interface, and even surpass the properties of the homogenous materials. Hence, multi-materials can be manufactured with FFF technique to manufacture functional materials without compromising mechanical properties. Going forward, microscopic or CT imaging will be utilized to examine the cross-section of the boundary interface in the overlap region, helping to understand how fibers contribute to improved adhesion. The lap shear strength of multiple specimens from each material combination will be depicted using box and whisker plots to assess test repeatability, including single variable ANOVA test which will establish a statistical correlation among the samples.

5 REFERENCES

[1] IEA (2021), *Global Energy Review* 2021, IEA, Paris https://www.iea.org/reports/global-energy-review-2021
[2] M. Gebler, *Energy Policy* **2014**, *74*, 158.
[3] E. C. Ehman, *J. Magn. Reson. Imaging* **2017**, *46*.
[4] T. Chen, *Sci. Rep.* **2017**, *7*, 45671.
[5] J. P. Moore, *Rapid Prototyp. J.* **2015**, *21*, 675.
[6] M. Sugavaneswaran, *Mater. Des. 1980-2015* **2014**, *54*, 779.
[7] M. Sugavaneswaran, *Mater. Des. 1980-2015* **2015**, *66*, 29.
[8] L. S. Dimas, *Adv. Funct. Mater.* **2013**, *23*, 4629.
[9] B. Berman, *Bus. Horiz.* **2012**, *55*, 155.
[10] M. Ribeiro, *Rapid Prototyp. J.* **2019**, *25*, 38.
[11] L. R. Lopes, *Addit. Manuf.* **2018**, *23*, 45.
[12] ASTM D5573-99(2019).